An Integrated Nine-Switch Power Conditioner for Power Quality Enhancement and Voltage Sag Mitigation

Lei Zhang, Poh Chiang Loh, *Member, IEEE*, and Feng Gao, *Member, IEEE*

Abstract—A nine-switch power converter having two sets of output terminals was recently proposed in place of the traditional back-to-back power converter that uses 12 switches in total. The nine-switch converter has already been proven to have certain advantages, in addition to its component saving topological feature. Despite these advantages, the nine-switch converter has so far found limited applications due to its many perceived performance tradeoffs like requiring an oversized dc-link capacitor, limited amplitude sharing, and constrained phase shift between its two sets of output terminals. Instead of accepting these tradeoffs as limitations, a nine-switch power conditioner is proposed here that virtually "converts" most of these topological short comings into interesting performance advantages. Aiming further to reduce its switching losses, an appropriate discontinuous modulation scheme is proposed and studied here in detail to doubly ensure that maximal reduction of commutations is achieved. With an appropriately designed control scheme then incorporated, the nine-switch converter is shown to favorably raise the overall power quality in experiment, hence justifying its role as a power conditioner at a reduced semiconductor cost.

Index Terms—Discontinuous pulse-width modulation, nine-switch converter, power conditioner, power quality.

Fig. 1. Representations of (a) back-to-back and (b) nine-switch power conditioners.

I. INTRODUCTION

SINCE its first introduction, static power converter development has grown rapidly with many converter topologies now readily found in the open literature. Accompanying this development is the equally rapid identification of application areas, where power converters can contribute positively toward raising the overall system quality [1], [2]. In most cases, the identified applications would require the power converters to be connected in series [3] or shunt [4], depending on the operating scenarios under consideration. In addition, they need to

be programmed with voltage, current, and/or power regulation schemes so that they can smoothly compensate for harmonics, reactive power flow, unbalance, and voltage variations. For even more stringent regulation of supply quality, both a shunt and a series converter are added with one of them tasked to perform voltage regulation, while the other performs current regulation. Almost always, these two converters are connected in a back-to-back configuration [5], using 12 switches in total and sharing a common dc-link capacitor, as reflected by the configuration drawn in Fig. 1(a). Where available, a microsource can also be inserted to the common dc link, if the intention is to provide for distributed generation in a microgrid [6], without significantly impacting on the long proven proper functioning of the back-to-back configuration.

Even though facing no major operating concerns at present, improvements through topological modification or replacement of the back-to-back configuration to reduce its losses, component count, and complexity would still be favored, if there is no or only slight expected tradeoff in performance. A classical alternative that can immediately be brought out for consideration is the direct or indirect matrix converter, where 18 switches are used in total. That represents six switches more than the back-to-back configuration, but has the advantage of removing

the intermediate electrolytic capacitor for compactness and lifespan extension. If the heavy switch count is still of concern, those indirect sparse matrix converters proposed in [7], [8] can be considered, where the minimum switch count attainable is nine, but at the expense of supporting only unidirectional power flow. Neither storage capacitor nor dc microsource is again needed, which thus renders the normal and sparse matrix converters as not the preferred choice, if ride-through is a requirement. Matrix converters are also not preferred, if voltage buck and boost operations are both needed for a specified direction of power flow.

Yet another reduced semiconductor topology can be found in [9], where the B4 converter is introduced for dc–ac or ac–dc energy conversion. The B4 converter uses four switches to form two phase legs with its third phase drawn from the midpoint of a split dc capacitive link. For tying two ac systems together, two B4 converters are needed with their split dc link shared [10]. The total number of switches needed is thus 8, which probably is the minimum achievable for interfacing two ac systems. The resulting ac–dc–ac converter should then be more rightfully referred to as the B8 converter. The B8 converter is, however, known to suffer from large dc-link voltage variation, unless both systems are of the same frequency and synchronized so that no fundamental current flows through the dc link. That certainly is a constraint, in addition to the lower ac voltage that can be produced by each B4 converter from its given dc-link voltage.

Overcoming some limitations of the B8 converter is the five-leg converter introduced in [11], which conceptually can be viewed as adding a fifth phase leg to the B8 converter. The added phase leg is shared by the two interfaced ac systems with now no large fundamental voltage variation observed across its dc link. The only constraint here is the imposition of common frequency operation on the two interfaced ac systems, which then makes it unsuitable for applications like utility powered adjustable speed drives and series-shunt power conditioners.

Presenting a better reduced semiconductor alternative for high quality series–shunt compensation, this paper proposes a single-stage integrated nine-switch power conditioner, whose circuit connection is shown in Fig. 1(b). As its name roughly inferred, the proposed conditioner uses a nine-switch converter with two sets of output terminals, instead of the usual 12 switch back-to-back converter. The nine-switch converter was earlier proposed in [12] and [13] at about the same time, and was recommended for dual motor drives [14], rectifier–inverter systems, and uninterruptible power supplies [15]. Despite functioning as intended, these applications are burdened by the limited phase shift and strict amplitude sharing enforced between the two terminal sets of the nine-switch converter.

More importantly, a much larger dc-link capacitance and voltage need to be maintained, in order to produce the same ac voltage amplitudes as for the back-to-back converter. Needless to say, the larger dc-link voltage would overstress the semiconductor switches unnecessarily, and might to some extent overshadow the saving of three semiconductor switches made possible by the nine-switch topology. The attractiveness of the nine-switch converter, if indeed any, is therefore not yet fully brought out by those existing applications discussed in

[13]–[15]. Although follow-up topological extensions can subsequently be found in [16], where a Z-source network and alternative modulation schemes are introduced, they did not fully address those critical limitations faced by the nine-switch converter, and not its traditional back-to-back counterpart.

Investigating further by taking a closer view at those existing applications described earlier, a general note observed is that they commonly use the nine-switch converter to replace two shunt converters connected back-to-back. Such replacement will limit the full functionalities of the nine-switch converter, as explained in Section II. In the same section, an alternative concept is discussed, where the nine-switch converter is chosen to replace a shunt and a series converter found in an integrated power conditioner, instead of two shunt converters. Underlying operating principles are discussed comprehensively to demonstrate how such "series–shunt" replacement can bring forth the full advantages of the nine-switch converter, while yet avoiding those limitations faced by existing applications. Details explaining smooth transitions between normal and sag operating modes are also provided to clarify that the more restricted nine-switch converter will not underperform the more independent back-to-back converter even for sag mitigation.

Section III then proceeds to compare the ratings and losses of the back-to-back and nine-switch conditioners, before an appropriate modulation scheme is evaluated in Section IV for reducing the nine-switch converter commutation count, and hence its switching losses. Also presented in Section IV is two sets of higher level control schemes with the first used for controlling one set of three-phase outputs so as to compensate for harmonic currents, reactive power flow and three-phase unbalance caused by nonlinear loads. The grid currents drawn from the utility are then sinusoidal, having only fundamental component. In synchronism, the second set of outputs is controlled to compensate for any detected grid voltage harmonics and unbalance, so that only a set of balanced three-phase voltages appears across the loads under normal operating conditions [17]. During voltage sags, the second set of control schemes also has the ability to continuously keep the load voltages within tolerable range. This sag mitigation ability, together with other conceptual findings discussed in this paper but not in the open literature, has already been verified in experiment with favorable results observed.

II. System Description and Operating Principles of a Nine-Switch Power Conditioner

A. Back-to-Back Converter Limitations and Recommendation

Fig. 1(a) shows the per-phase representation of the common back-to-back unified power quality conditioner (UPQC), where a shunt converter is connected in parallel at the point-of-common-coupling (PCC), and a series converter is connected in series with the distribution feeder through an isolation transformer. The shunt converter is usually controlled to compensate for load harmonics, reactive power flow, and unbalance, so that a sinusoidal fundamental current is always drawn from the utility grid, regardless of the extent of load nonlinearity. Complementing, the series converter is controlled to block grid harmonics, so that a set of three-phase fundamental voltages always appears

across the load terminals [18]. Rather than the described, the inverse assignment of functionalities with the shunt converter regulating voltage and series converter regulating current is also possible, as demonstrated in [19]. Being so flexible, the UPQC is indeed an excellent "isolator," capable of promptly blocking disturbances from propagating throughout the system.

Despite its popularity, the back-to-back UPQC is nonetheless still complex and quite underutilized, even though it offers independent control of two decoupled converters. Its underutilization is mainly attributed to the series converter, whose output voltages are usually small, since only small amount of grid harmonics need to be compensated by it under normal steady-state conditions, especially for strong grids ($\vec{V}_{\text{SUPPLY}} \approx \vec{V}_{\text{LOAD}}$). Some typical numbers for illustration can be found in [17], where it is stated that the converter modulation ratio can be as low as 0.05×1.15 with triplen offset included, if the converter is sized to inject a series voltage of 1.15 p.u. during sag occurrence. Such a low modulation ratio gives rise to computational problems, which fortunately have already been addressed in [18], but not its topological underutilization aspect.

Resolving the topological aspect is, however, not so easy, especially for cases where the dc-link voltage must be shared and no new component can be added. Tradeoffs would certainly surface, meaning that the more reachable goal is to aim for an appreciable reduction in component count, while yet not compromising the overall utilization level by too much. Offering one possible solution then, this paper presents an integrated power conditioner, implemented using the nine-switch converter documented in [12], [13], rather than the traditional back-to-back converter. Before the nine-switch converter can be inserted though, its impact should be thoroughly investigated to verify that there would not be any overburdening of system implementation cost and performance. This recommendation is advised as important, since earlier usages of the nine-switch converter for motor drives and rectifier–inverter systems have so far resulted in some serious limitations, which would be brought up for discussion shortly to highlight certain insightful concepts.

B. Nine-Switch Converter Operating Principles and Existing Constraints

As illustrated in Fig. 1(b), the nine-switch converter is formed by tying three semiconductor switches per phase, giving a total of nine for all three phases. The nine switches are powered by a common dc link, which can either be a microsource or a capacitor depending on the system requirements under consideration. Like most reduced component topologies, the nine-switch converter faces limitations imposed on its assumable switching states, unlike the fully decoupled back-to-back converter that uses 12 switches. Those allowable switching states can conveniently be found in Table I, from which, it is clear that the nine-switch converter can only connect its two output terminals per phase to either V_{dc} or 0 V, or its upper terminal to the upper dc rail P and lower terminal to the lower dc rail N. The last combination of connecting its upper terminal to N and lower terminal to P is not realizable, hence constituting the first limitation faced by the nine-switch converter. That limitation is

TABLE I
SWITCH STATES AND OUTPUT VOLTAGES PER PHASE

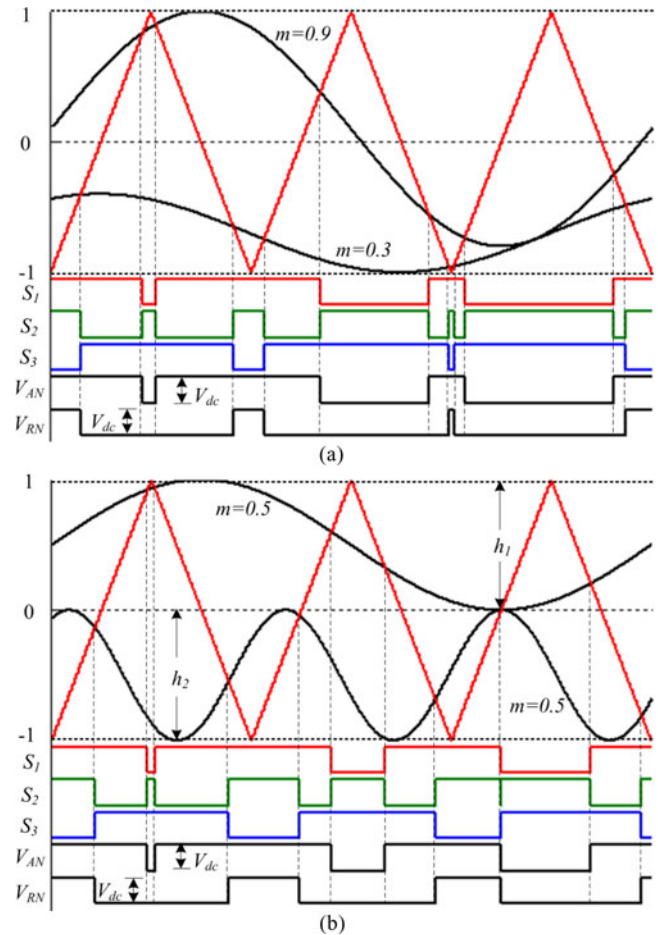| S_1	S_2	S_3	V_{AN}	V_{RN}
ON	ON	OFF	V_{dc}	V_{dc}
ON	OFF	ON	V_{dc}	0
OFF	ON	ON	0	0

Fig. 2. Arrangements of references having (a) the same frequency but different amplitudes, and (b) different frequencies but the same amplitude.

nonetheless not practically detrimental, and can be resolved by coordinating the two modulating references per phase, so that the reference for the upper terminal is always placed above that of the lower terminal, as per the two diagrams drawn in Fig. 2.

Imposing this basic rule of thumb on reference placement then results in those gating signals drawn in Fig. 2 for the three switches of S_1, S_2, and S_3 per phase. Equations for producing them can also be explicitly stated as

$$S_1 = !S_1' = \begin{cases} \text{ON}, & \text{if upper reference is larger than carrier} \\ \text{OFF}, & \text{otherwise} \end{cases}$$

$$S_3 = !S_3' = \begin{cases} \text{ON}, & \text{if lower reference is smaller than carrier} \\ \text{OFF}, & \text{otherwise} \end{cases}$$

$$S_2 = S_1' \oplus S_3' \tag{1}$$

where $\oplus$ is the logical XOR operator. Signals obtained from (1), when applied to the nine-switch converter, then lead to
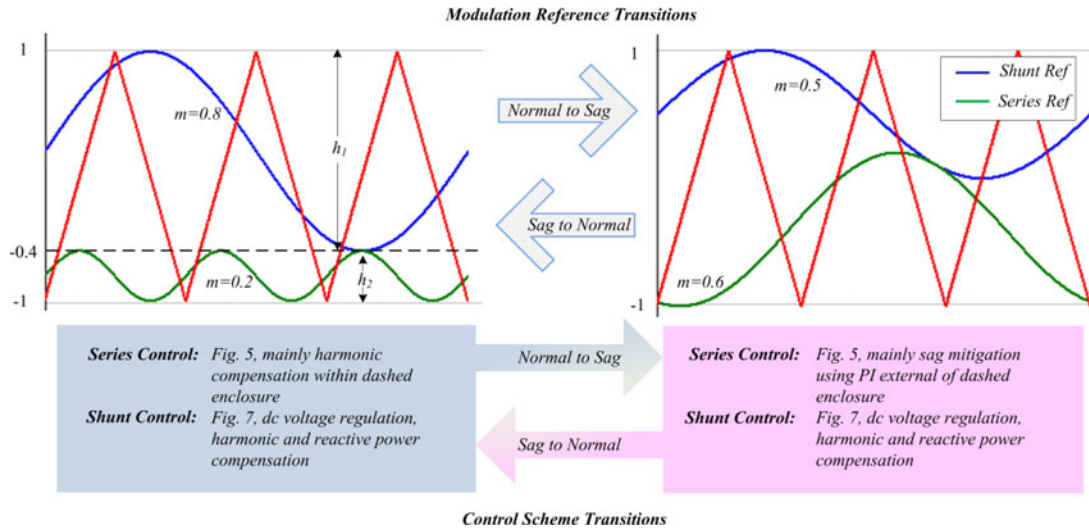
Fig. 3.   Transitions of modulating references and control schemes between normal (left) and sag mitigation (right) modes.

those output voltage transitional diagrams drawn in Fig. 2 for representing V_{AN} and V_{RN} per phase. Together, these voltage transitions show that the forbidden state of $V_{AN} = 0\,\text{V}$ and $V_{RN} = V_{\text{dc}}$ is effectively blocked off. The blocking is, however, attained at the incurrence of additional constraints limiting the reference amplitudes and phase shift. These limitations are especially prominent for references having sizable amplitudes and/or different frequencies, as exemplified by the illustrative cases shown in Fig. 2(a) and (b). In particular, Fig. 2(a) shows two references of common frequency limited in their phase displacement, while Fig. 2(b) shows two references of different frequencies limited to a maximum modulation ratio of 0.5 each, extendible by 1.15 times if triplen offset is added, in order to avoid crossover. The limited phase-shift constraint, associated with references of the same frequency and combined modulation ratio of greater than 1.15 with triplen offset added (=1.2 in Fig. 2(a) as an example), has recently been shown to adapt well with online uninterruptible power supplies [15], which indeed is a neat and intelligent application of the nine-switch converter. This, however, is only a single application, which by itself is not enough to bring forward the full potential of the nine-switch converter.

Considering now the second limitation detailed in Fig. 2(b), a helpful example for explaining it is the nine-switch dual drive system proposed in [13], where references used for modulation can have different operating frequencies. These references are for the two output terminal sets of the nine-switch converter, tied to separate motors operating at approximately the same rated voltage but at different frequencies. Such motor operating criteria would force the references to share the common carrier range equally, like that drawn in Fig. 2(b). The maximum modulation ratio allowed is therefore 0.5×1.15 per reference. Even though technically viable, such sharing of carrier is not practically favorable, since to produce the same output voltages, the dc-link voltage maintained, and hence semiconductor stress experienced, must at least be doubled. Doubling of voltage is, however, not needed for the traditional dual converter, whose topological structure is similar to the back-to-back converter,

and hence would also support a maximum modulation ratio of unity. Quite clearly then, doubling of dc-link voltage is attributed to the halving of modulation ratios imposed by the nine-switch converter, and is therefore equally experienced by the ac–dc–ac adjustable speed motor drives recommended in [14], where the nine-switch converter is again operating at different frequencies.

Judging from these examples, the general impression formed is that the nine-switch converter is not too attractive, since its semiconductor saving advantage is easily shadowed by tradeoffs, especially for cases of different terminal frequencies. Such unattractiveness is however not universal, but noted here to link only with those existing applications reported to date, where the nine-switch converter is used to replace two shunt-connected converters. References demanded by these shunt converters are usually both sizable, inferring that the carrier band must be shared equally between them, and hence giving rise to those tradeoffs identified earlier. Therefore, instead of "shunt–shunt" replacement, it is recommended here that the nine-switch converter should more appropriately be used for replacing a series and a shunt converter like those found in a power quality conditioner or any other "series–shunt" topological applications. Explanation for justifying that recommendation is provided in Section II-C with all relevant advantages and residual tradeoffs identified.

C. Proposed Nine-Switch Power Conditioner

Under normal operating conditions, the output voltage amplitude of the shunt converter is comparatively much larger than the voltage drop introduced by the series converter along the distribution feeder. That indirectly means the modulating reference needed by the shunt converter is much larger than that associated with the series converter, which might simply consist of only the inverse harmonic components for grid voltage compensating purposes. Drawing these details in the carrier range would then result in a much wider vertical range h_1 in the left diagram of Fig. 3 for controlling the upper shunt terminal, and a narrower h_2 for controlling the lower series terminal ($h_1 \gg$

h_2). Other operating details like logical equations used for generating gating signals for the three switches per phase would remain unchanged, as per (1).

For h_2, a comment raised here is that it can be set to zero, if an ideal grid with no distortion and rated sinusoidal voltage is considered. In that case, the lowest three switches, labeled as S_3 for each phase in Fig. 1(b), should always be kept ON to short out the series coupling transformer, and to avoid unnecessary switching losses. If desired, the series transformer can also be bypassed at the grid side to remove unwanted leakage voltage drop without affecting the compensating ability of the shunt converter. Tailored operation with an ideal grid is therefore possible, as described, but for modern grids with abundant distributed nonlinear loads, voltage distortion is relatively common, since any amount of harmonic load current flowing through a finite line or transformer impedance would have caused voltage at the PCC to be distorted. Series harmonic compensation of the grid or PCC voltage is therefore technically needed, and hence included here for discussion, if a smoother load voltage is demanded.

Referring back to the h_1 and h_2 carrier band division shown in the left illustration of Fig. 3, it would still need a higher dc-link voltage as a tradeoff in the UPQC, but the increase is much reduced, and definitely not anywhere close to doubling. Quoting [17] as an example, where a modulation ratio of the series converter can be as low as 0.05×1.15 with triplen offset included, the increase in dc-link voltage is merely about 5%, before the same maximum shunt voltage amplitude, like in a back-to-back converter, can be produced by the nine-switch converter. This maximum is however arrived at a reduced maximum modulation ratio of 0.95×1.15, instead of 1.15 with triplen offset considered. The scenario would somehow be improved slightly, if an ideal grid is considered instead, in which case, h_2 is set to zero, as explained in an earlier paragraph. No increase in dc-link voltage is then needed, and the maximum shunt voltage amplitude can be produced at a modulation ratio of 1.15. Replacing of "series–shunt" converter by the nine-switch converter is, therefore, an acceptable option with its saving of three semiconductor switches viewed here as more profound, since they represent heavily underutilized switches found in the back-to-back converter for series compensation purposes.

Yet another issue to address, before the nine-switch converter can be confirmed as a favorable topology for the "series–shunt" power conditioner, is to study its compensating ability under voltage sag condition. For that purpose, the PCC voltage in Fig. 1(b) is assumed to dip by some amount, which would then subject the higher shunt terminal of the nine-switch converter to a reduced voltage level. In contrast, the lower series terminal must respond immediately by injecting a sizable series voltage at the fundamental frequency ($\vec{V}_{\text{SERIES}} = \vec{V}_{\text{LOAD}}^* - \vec{V}_{\text{SUPPLY}}$, where $\vec{V}_{\text{LOAD}}^*$ is the demanded load voltage reference), so as to keep the load voltage close to its prefault value.

Updating this sag operating scenario to the carrier domain then results in the shunt terminal using a reduced reference, and the series terminal widening its reference range to include a sizable fundamental component, regardless of whether h_2 is

initially zero for an ideal grid or taking a small value for a distorted grid. Since both references are now predominantly fundamental with sizable amplitudes, their placement can ended up like the example drawn on the right of Fig. 3 with the same earlier mentioned phase-shift limitation imposed. Fortunately, this limitation will not hinder the operation of the nine-switch conditioner, since large injected series voltage with a demanding phase shift is usually accompanied by a severe sag at the PCC, and hence a much reduced shunt modulating reference. The compressed shunt reference would then free up more carrier space below it for the series reference to vary within, as easily perceived from the example drawn on the right of Fig. 3.

In conclusion, the proposed nine-switch power conditioner can indeed operate well under both normal and sag operating conditions, owing to its autocomplementary tuning of shunt and series references within the single common carrier band. Suitability of the nine-switch converter for "series–shunt" replacement is therefore established without any stringent practical limitations encountered, unlike those existing "shunt–shunt" replacements.

III. PER UNIT COMPARATIVE DETAILS

Section II-C provides a qualitative justification for using the nine-switch converter as a UPQC or other series–shunt conditioners. This justification is now reinforced here by some numerical values calculated for determining the semiconductor losses and component ratings of the back-to-back and nine-switch power conditioners. For the latter, it is further divided into three subcategories without modifying the context of series–shunt power conditioning. The following now describes each of the four cases in detail, before summarizing their features in Table II.

A. Back-To-Back UPQC

Back-to-back UPQC allows independent control of its shunt and series converters, and hence does not need to divide its carrier band into two, like in Fig. 3. That means h_2 is zero, and its dc-link voltage can be set to the minimum of $V_{\text{dc}-\text{BB}} = 2\sqrt{2}/1.15$ p.u. (subscript BB stands for "back-to-back"), if the nominal RMS grid voltage is chosen as the base. Voltage ratings of the dc-link capacitor, series and shunt switches would thus have to be higher than this value, after adding some safety margin. Current rating of the series switches also has to be higher than $(1 + k)$ p.u., after adding some safety margin, and treating the nominal sinusoidal RMS load current as the base. The term k then represents the amount of load current "polluted" by low-order harmonic and reactive components, whose negation $-k$ represents the current flowing through the shunt switches, while performing load current compensation.

Rating of the shunt switches must however be larger than k p.u., so as to allow the shunt converter to channel enough energy to the series converter for onward transferring to the load during period of sag compensation, as would also be shown later through experimental testing. For that, the raised shunt value can be set equal to the series value of $(1 + k)$ p.u. for uniformity, or any other higher value that is deemed appropriate. Using these

TABLE II
P.U. COMPONENT RATINGS AND LOSSES NORMALIZED TO NOMINAL GRID VOLTAGE AND LOAD CURRENT

UPQC TYPE	Capacitor Voltage Rating	Semiconductor Voltage Rating	Semiconductor Current Rating	Total Semiconductor Losses (Conduction & Switching)
*** With Series Compensation ***				
Back-to-Back UPQC	$2\sqrt{2}/1.15$	$2\sqrt{2}/1.15$	$1+k$	4.62% Normal; 5.40% Sag[1]
Proposed Nine-Switch UPQC	$1.05 \times 2\sqrt{2}/1.15$	$1.05 \times 2\sqrt{2}/1.15$	$1+k$	3.24% Normal; 5.19% Sag[1]
Nine-Switch UPQC with Equally Divided Carrier	$2 \times 2\sqrt{2}/1.15$	$2 \times 2\sqrt{2}/1.15$	$1+k$	9.26% Normal; 11.27% Sag[1]
*** Without Series Compensation ***				
Back-to-Back UPQC	$2\sqrt{2}/1.15$	$2\sqrt{2}/1.15$	$1+k$	0.62% Normal; 5.40% Sag[1]
Nine-Switch UPQC with CF Control	$2\sqrt{2}/1.15$	$2\sqrt{2}/1.15$	$1+k$	0.71% Normal; 4.94% Sag[1]

[1]Evaluated with a 40% in-phase sag

identified values, the overall losses of the back-to-back conditioner are determined using the same simulation approach and parameters for the 600 V/50 A insulated gate bipolar transistor (IGBT) presented in [12]. Other IGBT parameters can certainly be used, but by using the same parameters as in [12], a firm foundation for result verification is formed without compromising generality. Results obtained are subsequently tabulated in Table II for later comparison purposes.

B. Proposed Nine-Switch UPQC

As shown in Fig. 3, the proposed nine-switch UPQC operates with its carrier band divided into h_1 and h_2. The latter, being much narrower, is for blocking small grid harmonic voltages from propagating to the load, which from the example described in [17], is only about 5% of the full carrier band. The minimum dc-link voltage, and hence voltage ratings of components, must then be chosen based on $V_{\text{dc-NS}} = 1.05\, V_{\text{dc-BB}}$, where subscript *NS* is used to represent "nine-switch." Current rating wise, analysis of the nine-switch UPQC is slightly different, because of its merging of functionalities to gain a reduction of three switches.

Focusing first at the upper S_1 switch, maximum current flowing through it would be the sum of shunt ($-k$) and series ($1 + k$) currents per phase when S_1 and S_2 are turned ON, and hence giving a final value of 1 p.u. Being slightly higher, the common maximum current flowing through S_2 and S_3 is $(1 + k)$ p.u., which flows when S_1 and S_2 are turned ON for the former, and S_1 and S_3 are turned ON for the latter. Note, however that these maximum currents are only for sizing the switches, and should not be exclusively used for computing losses. The reason would be clear after considering S_1 as an example, where it is noted that the maximum current of 1 p.u. does not always flow. In fact, when S_1 and S_3 are turned ON, the current flowing through S_1 is smaller at $-k$ p.u., whose duration depends on a number of operating parameters like modulation ratio, phase displacement, and others. Analytical computation of losses is therefore nontrivial, as also mentioned in [12], whose simulation approach is now practiced here for computing the UPQC losses. Obtained results for both normal and sag operating modes are subsequently summarized in Table II for easier referencing.

C. Nine-Switch UPQC with Only Common Frequency Control

Nine-switch UPQC, constrained to operate with the same common frequency (CF) at its shunt and series terminals, is not able to compensate for harmonic grid voltages. Parameter h_2 in Fig. 3 is therefore redundant, and can be set to zero, whose effect is a minimum dc-link voltage that is no different from that of the back-to-back UPQC. The series transformer, being no longer used, can also be bypassed to avoid unnecessary leakage voltage drop, and to divert the large load current away from the UPQC, leaving the three switches per phase to condition only the $-k$ shunt current. Among the switches, the lowest S_3 switch behaves differently in the sense that it is always turned ON, as explained in Section II-C, and therefore produces only conduction losses. It will only start to commutate when a sag occurs, and the transformer exists its bypassed state. When that happens, the load current again flows through the switches, inferring that their current rating must still be chosen above $(1 + k)$ p.u., as reflected in Table II, together with some calculated loss values.

D. Nine-Switch UPQC with Equal Division of Carrier Band

Although not encouraged, the nine-switch UPQC can also be implemented with its carrier band divided into two equal halves, like the different frequency mode studied previously in [12]–[14]. The maximum modulation ratio per reference is then 0.5×1.15, whose accompanied effect is the doubling of dc-link voltage and switch voltage rating without affecting their corresponding current rating. Such doubling is of course undesirable, which fortunately can be resolved for UPQC and other series–shunt applications, by simply dividing the carrier band appropriately with h_1 being much wider than h_2, instead of making them equal. Results for the latter, although not recommended, are still added to Table II for comprehensiveness.

E. Comparative Findings

Analyzing all results tabulated in Table II, it is clear that the higher voltage requirement of the nine-switch UPQC can be as much as doubled, if not implemented correctly. This doubling can fortunately be reduced by narrowing the half, labeled as h_2 in Fig. 3, to only 5% of the full carrier band. Another observation

noted is the slightly lower losses of the nine-switch UPQC, as compared to its back-to-back precedence, when both schemes have their series compensation activated. The same lower losses are also observed with voltage sag mitigation, but not with equal carrier division. The latter in fact causes losses to more than doubled, because of the doubled dc-link voltage and higher rated IGBT used for implementation.

The same calculation can again be performed with no series compensation included. For the nine-switch UPQC, it just means the CF mode discussed in Section III-C with h_2 set to zero and the transformer bypassed. The former leads to a smaller dc-link voltage, while the latter causes losses to be smaller, since large load current now does not flow through the nine-switch UPQC. For comparison, values calculated for the back-to-back UPQC operating without series compensation are also included, which clearly show it having slightly lower losses under normal operating condition. The lower losses here are attributed to the back-to-back UPQC using only six modulated switches for shunt compensation, while the nine-switch UPQC uses six upper modulated switches (S_1 and S_2 per phase) and three lower conducting switches (S_3). This finding would reverse when sag occurs, during which the back-to-back UPQC uses 12 modulated switches, while the nine-switch UPQC uses only nine, and hence producing lower losses.

IV. MODULATION AND CONTROL

Upon verifying its appropriateness, suitable modulation and control schemes are now presented for controlling the nine-switch UPQC with reduced switching losses and roughly the same performance standards as its back-to-back counterpart. Relevant details for attaining these goals are presented shortly in Section IV-A–C.

A. Modulation Principles

Because of its independency, modulation of traditional back-to-back converter can be performed with its two sets of three-phase references centrally placed within the vertical carrier span. Performance quality obtained would then be comparable to the optimal space vector modulation (SVM) scheme. Such central placement is, however, not realizable with the nine-switch power conditioner, whose references must be placed one above the other, as explained in Section II-B. Obtaining optimal waveform quality at both terminals of the nine-switch converter is, therefore, not possible, but is not a serious limitation, since modern semiconductor devices and power conversion techniques would have greatly diluted the spectral gains introduced anyway.

Being unrealizable and insignificant, the objective set for modulating the nine-switch converter should rightfully not be spectral gain, but rather a reduction in switching losses. With the latter objective in mind, the immediate modulation choices for consideration would likely be from those traditional discontinuous modulation schemes, like the popular 60°- and 30°-discontinuous schemes [20]. Upon evaluation though, these schemes (60°- and 30°-discontinuous) are found to be not suitable for the nine-switch converter, since they require both upper and lower dc-rail clamping per set of output terminals, which
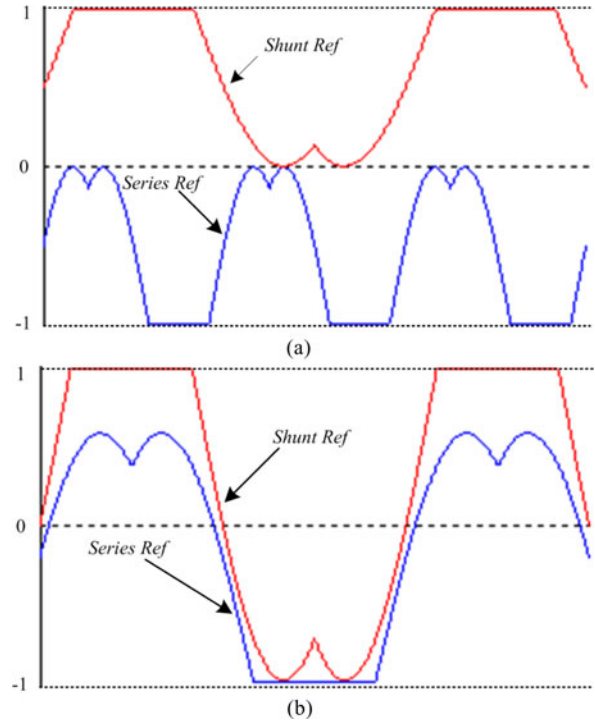

Fig. 4. 120°-discontinuous references with (a) $M_{SH} = M_{SE} = 0.5$, $\omega_{SH} \neq \omega_{SE}$, and (b) $M_{SH} = 1 \times 1.15$, $M_{SE} = 0.8 \times 1.15$, $\omega_{SH} = \omega_{SE}$.

technically cannot be met by the nine-switch converter. Instead, the nine-switch converter only allows upper dc-rail clamping for its upper terminals, and lower dc-rail clamping for its lower terminals, which so far can only be met by the less commonly adopted 120°-discontinuous modulation scheme.

To formally demonstrate its suitability, relevant offset and modified reference expressions for the 120°-discontinuous modulation scheme are derived, and listed in (2), before plotting them in Fig. 4 for illustration of one phase.

Sinusoidal References

$$\begin{cases} V_A = M_{SH} \cos(\omega_{SH}t + \theta_{SH}) \\ V_B = M_{SH} \cos(\omega_{SH}t - 120° + \theta_{SH}) \\ V_C = M_{SH} \cos(\omega_{SH}t + 120° + \theta_{SH}) \end{cases}$$

$$\begin{cases} V_R = M_{SE} \cos(\omega_{SE}t + \theta_{SE}) \\ V_Y = M_{SE} \cos(\omega_{SE}t - 120° + \theta_{SE}) \\ V_W = M_{SE} \cos(\omega_{SE}t + 120° + \theta_{SE}) \end{cases}$$

120°-Discontinuous Modified References

$$V'_\gamma = V_\gamma + V_{SH}, \quad V_{SH} = 1 - \max(V_A, V_B, V_C)$$

$$\gamma = A, B, \text{ or } C$$

$$V'_\partial = V_\partial + V_{SE}, \quad V_{SE} = -1 - \min(V_R, V_Y, V_W)$$

$$\partial = R, Y, \text{ or } W \tag{2}$$

where $\{M_{SH}, \omega_{SH}, \theta_{SH}\}$ are the modulation ratio, angular frequency, and initial phase of the shunt terminals, and $\{M_{SE}, \omega_{SE}, \theta_{SE}\}$ are the corresponding quantities for the series terminals.
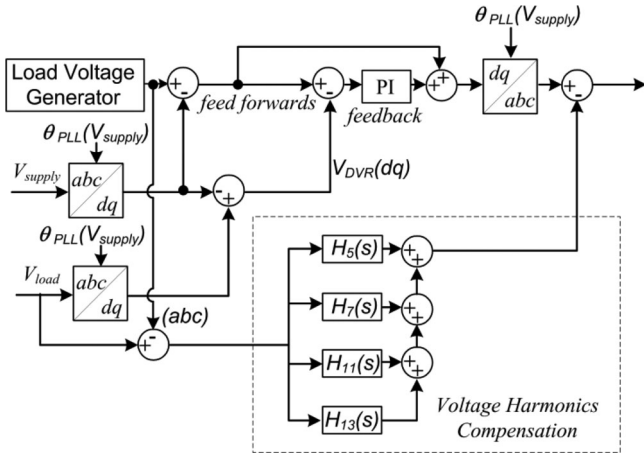
Fig. 5.   Series control block representation.

Fig. 6.   Bode representation of the selective harmonic regulators found in the series control scheme.

Using (2), the modulation plots obtained in Fig. 4 clearly show the upper reference tied to only the upper dc-rail and lower reference tied to only the lower dc-rail for a continuous duration of 120° per fundamental cycle. No crossover of references is observed, implying that the basic modulation rule-of-thumb of the nine-switch converter is not breached, and the 120°-discontinuous scheme is indeed a suitable scheme for reducing its commutation count by 33%. Lower commutation count would then lead to lower switching losses, whose values depend on the current amplitudes and phases at the two terminals per phase, like all other converters modulated discontinuously.

Before proceeding on to Sections IV-A and IV-B on higher level control, it is fair to comment here that a similar modulation scheme can be found in [21], whose derivation is oriented more toward the space vector approach. Surely, the space vector domain can be insightful, but it also needlessly complicates the modulation process, and does not bring out the clamping patterns between the two references per phase as clearly as the carrier-based approach. The latter is therefore preferred, and has independently been used by the authors to develop the 120°-discontinuous scheme, first presented in [22].

B. Series Control Principles

The series terminals of the nine-switch UPQC are given two control functions that can raise the quality of power supplied to the load under normal and sag operating conditions. For the former, the series terminals of the conditioner are tasked to compensate for any harmonic distortions that might have originated at the PCC. Where necessary, they should also help to regulate the load voltage to compensate for any slight fundamental voltage variation. This second functionality is, however, more relevant under voltage sag condition, where a sizable series voltage ($\vec{V}_{\text{SERIES}} = \vec{V}_{\text{LOAD}}^* - \vec{V}_{\text{SUPPLY}}$) needs to be injected to keep the load voltage nearly constant. The overall control block representation realized is shown in Fig. 5, where the subsystem responsible for voltage harmonic compensation is distinctly identified within the rectangular enclosure.

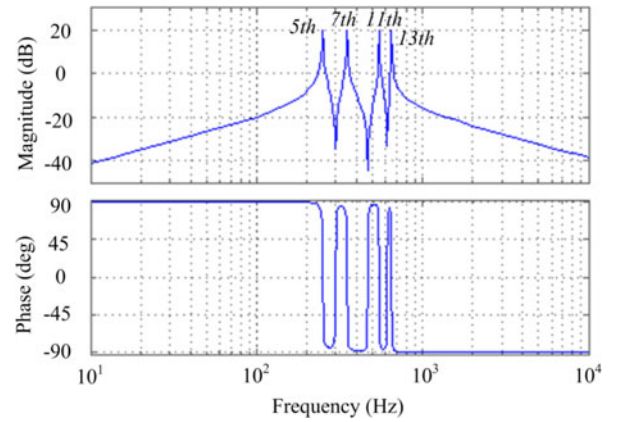As seen, the harmonic compensation subsystem is realized by including multiple resonant regulators in the stationary frame for singling out those prominent low-order load voltage harmonics, including the 5th, 7th, 11th, and 13th components, for elimination. Transfer functions representing these resonant regulators $H_n(s)$ and their illustration in the Bode diagram are given in (3) and Fig. 6, respectively [23]

$$H_n(s) = 2K_I\omega_c \frac{s + \omega_c}{s^2 + 2\omega_c s + \omega_n^2 + \omega_c^2} \qquad (3)$$

where K_I, ω_n, and ω_c represent the gain parameter, chosen harmonic resonant frequency, and cutoff frequency introduced for raising stability, respectively, but at the expense of slight transient sluggishness.

From Fig. 6, it is certainly verified that the regulators introduce multiple high gain resonant peaks only at those chosen harmonic frequencies, with gains at the other frequencies close to zero. Selective harmonic compensation is therefore realizable, and has the advantage of reducing the burden shouldered by the power conditioner, given also that not all harmonics in the load voltage error need to be eliminated in the first place [17], [24]. Another advantage gained by realizing the regulators in the stationary frame is linked to the internal model concept, which hints that a single resonant regulator tuned at a certain frequency can process both positive- and negative-sequence components located at that frequency [25]. In contrast, if realized in the synchronous frame, two control paths per harmonic would generally be needed for processing positive- and negative-sequence components separately. Depending on the number of harmonics considered, such separate paths might end up overstressing the control circuit or microcontroller unnecessarily. To avoid these unwarranted complications, implementation in the stationary frame is therefore preferred, and would in fact suit the carrier-based modulation scheme presented in Section III-A better.

Upon next detecting the occurrence of voltage sag, the series control focus should rightfully switch from harmonic compensation to fundamental voltage restoration. Spontaneously, the series modulating reference fed to the pulse-width modulator would change from a small harmonic wave pattern to one with fundamental frequency and much larger amplitude, determined solely by the extent of voltage sag. This "normal-to-sag" reference transition has earlier been shown in Section II-C to be

TABLE III
LOAD VOLTAGE COMPENSATION RESULTS

	5th	7th	11th	13th	5th	7th	11th	13th
No Compensation	2.58%	2.79%	0.85%	1.35%	9.13%	5.59%	3.16%	2.39%
	THD = 4.18%				THD = 11.43%			
With Compensation	0.11%	0.34%	0.06%	0.46%	0.01%	0.39%	0.11%	0.70%
	THD = 0.92%				THD = 1.12%			

smooth, so long as the proper higher level control scheme for producing the demanded series modulating reference is in place.

Moving forward to explain the higher level control operation during sag, Fig. 5 is referred to again, where those sag compensating blocks shown above the harmonic regulators are now discussed. Upon analyzing those blocks, the sag compensator is noted to have two degrees of control freedom with the first primary degree formed by subtracting the PCC voltage from the demanded load voltage along the feedforward path to give $\vec{V}^*_{\text{LOAD}} - \vec{V}_{\text{SUPPLY}}$. Feeding forward of control signal is however not capable of compensating for voltage drops appearing across the filter and transformer. Because of that, a secondary feedback loop is added to act on the load voltage error, derived by subtracting the load voltage from its reference ($\vec{V}^*_{\text{LOAD}} - \vec{V}_{\text{LOAD}}$). The computed voltage error is then fed through a PI regulator in the synchronous frame, whose effect is to force the steady-state error to zero, and hence compensating for those unaccounted voltage drops appearing across the inductive elements.

Note that for the control presented here, the synchronous frame is chosen simply because the load voltage reference can then be represented by a single dc constant. If frame transformation is not preferred, resonant regulator in the stationary frame [26] can be used instead, so long as three-phase sinusoids are also used as the load voltage references.

C. Shunt Control Principles

As per previous power conditioners, the shunt terminals of the nine-switch power conditioner are programmed to compensate for downstream load current harmonics, reactive power, and to balance its shared dc-link capacitive voltage. To realize these control objectives, an appropriate control scheme is drawn in Fig. 7, where the measured load current is first fed through a high-pass filter in the synchronous frame. The filter blocks fundamental d-axis active component, and passes forward the harmonics and q-axis reactive component for further processing. In parallel, a PI regulator is also added to act on the dc-link voltage error, forcing it to zero by generating a small d-axis control reference for compensating losses, and hence maintaining the dc-link voltage constant. The sum of outputs from the filter and PI regulator then forms the control reference for the measured shunt current to track. Upon tracked properly, the source current would be sinusoidal, and the load harmonics and reactive power would be solely taken care of by the proposed power conditioner.
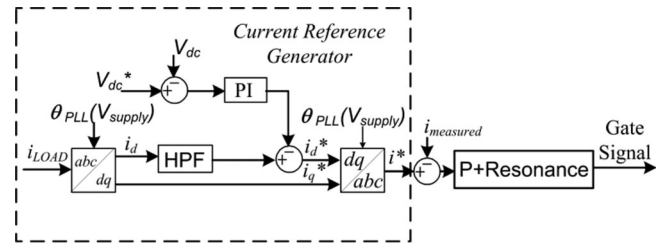

Fig. 7. Shunt control block representation.

V. EXPERIMENTAL VERIFICATION

To validate its performance, a nine-switch power conditioner was implemented in the laboratory, and controlled using a *dSPACE DS1103* controller card. The *dSPACE* card was also used for the final acquisition of data from multiple channels simultaneously, while a 4-channel Lecoy digital scope was simply used for the initial debugging and verification of the dSPACE recorded data, but only four channels at a time. The final hardware setup is shown in Fig. 8, where parametric values used are also indicated. Other features noted from the figure include the shunt connection of the upper UPQC terminals to the supply side, and the series connection of the lower terminals to the load side through three single-phase transformers. Reversal of terminal connections for the setup, like upper→series and lower→shunt, was also affected, but was observed to produce no significant differences, as anticipated. For flexible testing purposes, the setup was also not directly connected to the grid, but was directed to a programmable ac source, whose purpose was to emulate a controllable grid, where harmonics and sags were conveniently added.

With such flexibility built-in, two distorted cases were programmed with the first having a lower total harmonic distortion (THD) of around 4.18%. This first case, being less severe, represents most modern grids, regulated by grid codes, better. The second case with a higher THD of around 11.43% was included mainly to show that the nine-switch UPQC can still function well in a heavily distorted grid, which might not be common in practice. Equipped with these two test cases, experiments were conducted with the shunt compensation scheme shown in Fig. 7 always activated, so as to produce the regulated dc-link voltage needed for overall UPQC operation. The series compensation scheme shown in Fig. 5, on the other hand, was first deactivated, and then activated to produce the two sets of comparative load voltage data tabulated in Table III. The data obviously show that the proposed nine-switch UPQC is effective in smoothing the
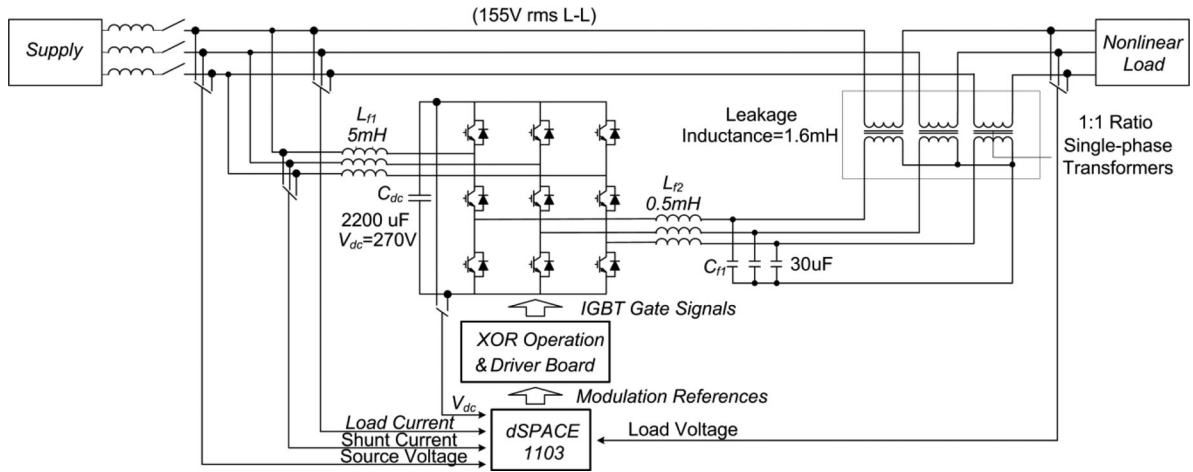
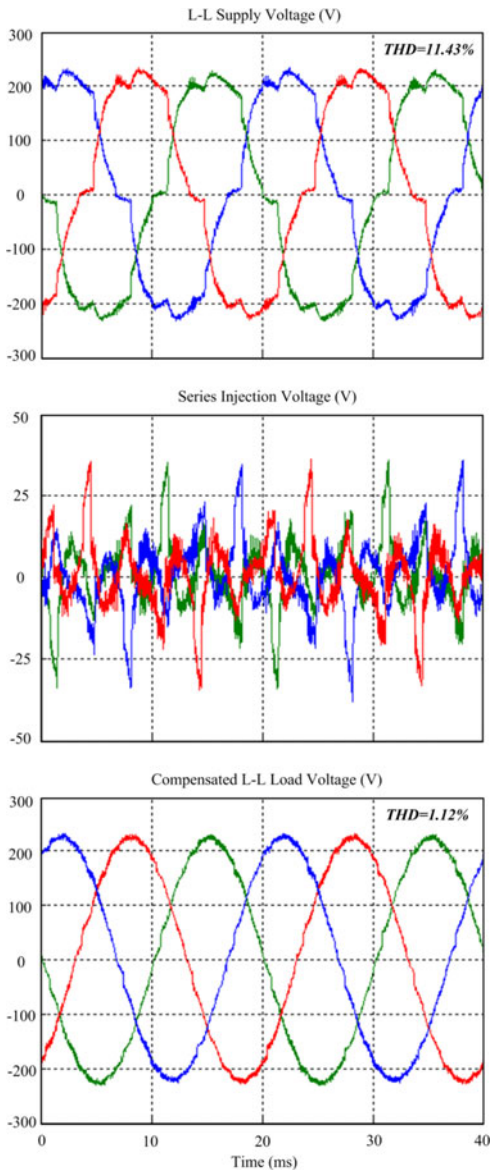Fig. 8.   Experimental setup and parameters used for testing.

Fig. 10.   Experimental source, shunt injection, and load currents captured during normal power conditioning mode.
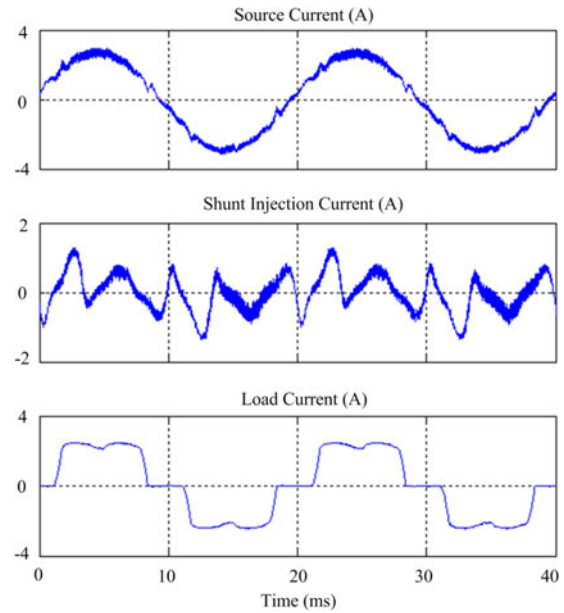

Fig. 9.   Experimental supply, series injection, and load voltages captured during normal power conditioning mode.

load voltage, regardless of the extent of low order grid harmonic distortion introduced.

To strengthen this observation, Fig. 9 shows the supply, series injection, and load voltages for the second test case with a higher grid THD, and with both series and shunt compensation activated. The supply voltage is indeed distorted, and would appear across the load if series compensation is deactivated and the transformer is bypassed. The distortion would, however, be largely blocked from propagating to the load, upon activating the series compensation scheme with the shunt compensation scheme still kept executing. Example load voltage waveform illustrating this effectiveness can be found at the bottom of Fig. 9.

Roughly, the same results were also obtained when the nine-switch converter was replaced by its back-to-back precedence with all other system parameters and control schemes kept
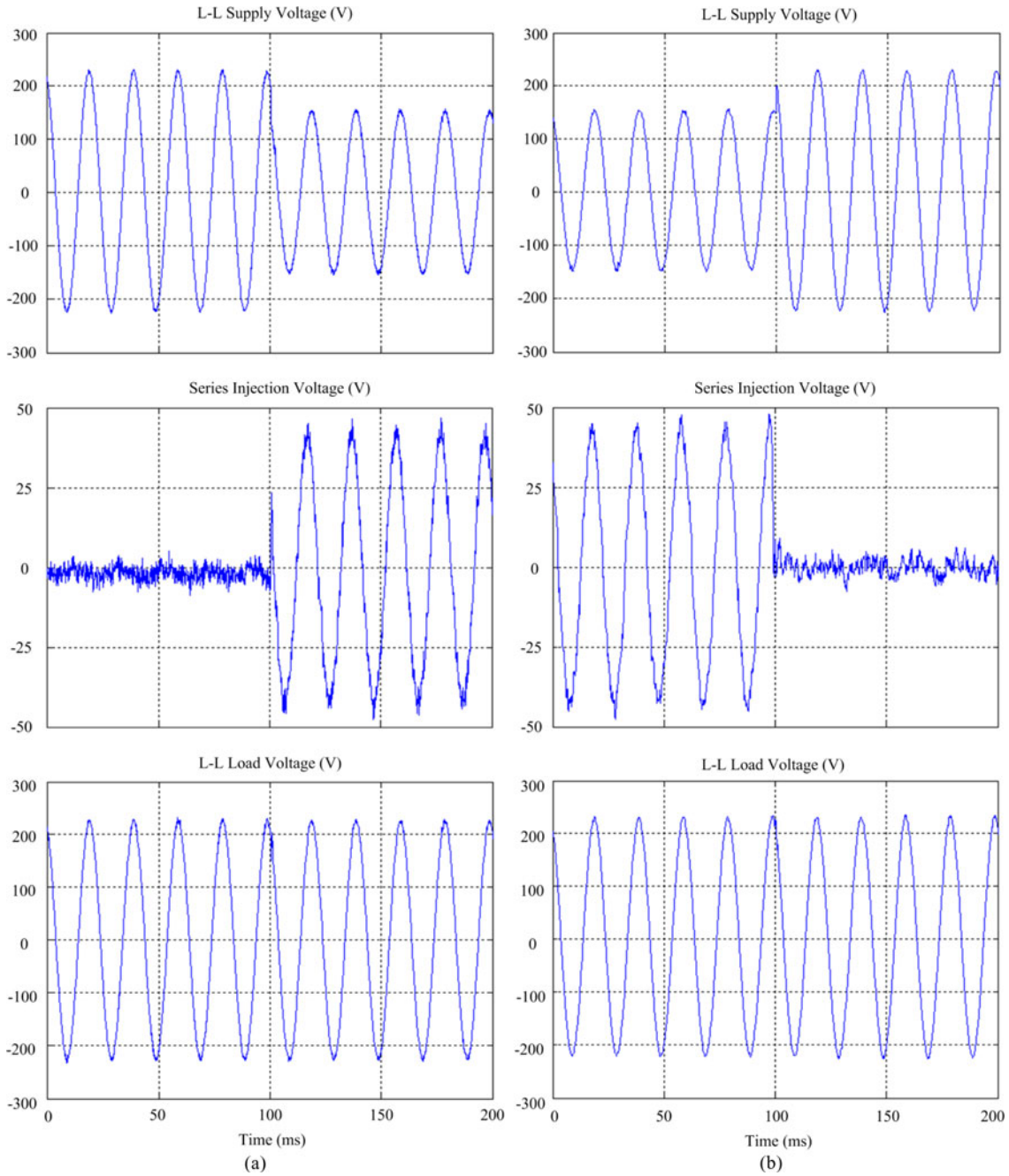
Fig. 11.   Experimental supply, series injection, and load voltages during (a) normal-to-sag and (b) sag-to-normal transitions.

unchanged. This finding is certainly expected, since both converters differ only by their high frequency switching harmonics produced, which will not be prominent in those filtered quantities of interest, shown in Table III and Fig. 9. Producing the same results is however still an advantage for the nine-switch converter, since it achieves that with three lesser semiconductor switches, and hence a lower system cost. To next verify its shunt compensating ability, Fig. 10 shows the source, shunt injection and load currents conditioned by the nine-switch UPQC. Although the load current is heavily distorted, the shunt control scheme in Fig. 7 is capable of compen-

sating it, so that the grid current drawn is always sinusoidal, as intended.

With the programmable source now configured to introduce a 20% sag, Fig. 11 shows the correspondingly sagged grid voltage, series injection voltage, and compensated load voltage during the normal to sag transition and its inverse recovery. These waveforms collectively prove that the sag has been blocked from propagating to the load, while yet using lesser semiconductor switches. Complementing, Fig. 12 shows the grid, shunt injection, and load currents during the same normal to sag transition and its recovery. The grid current is obviously sinusoidal
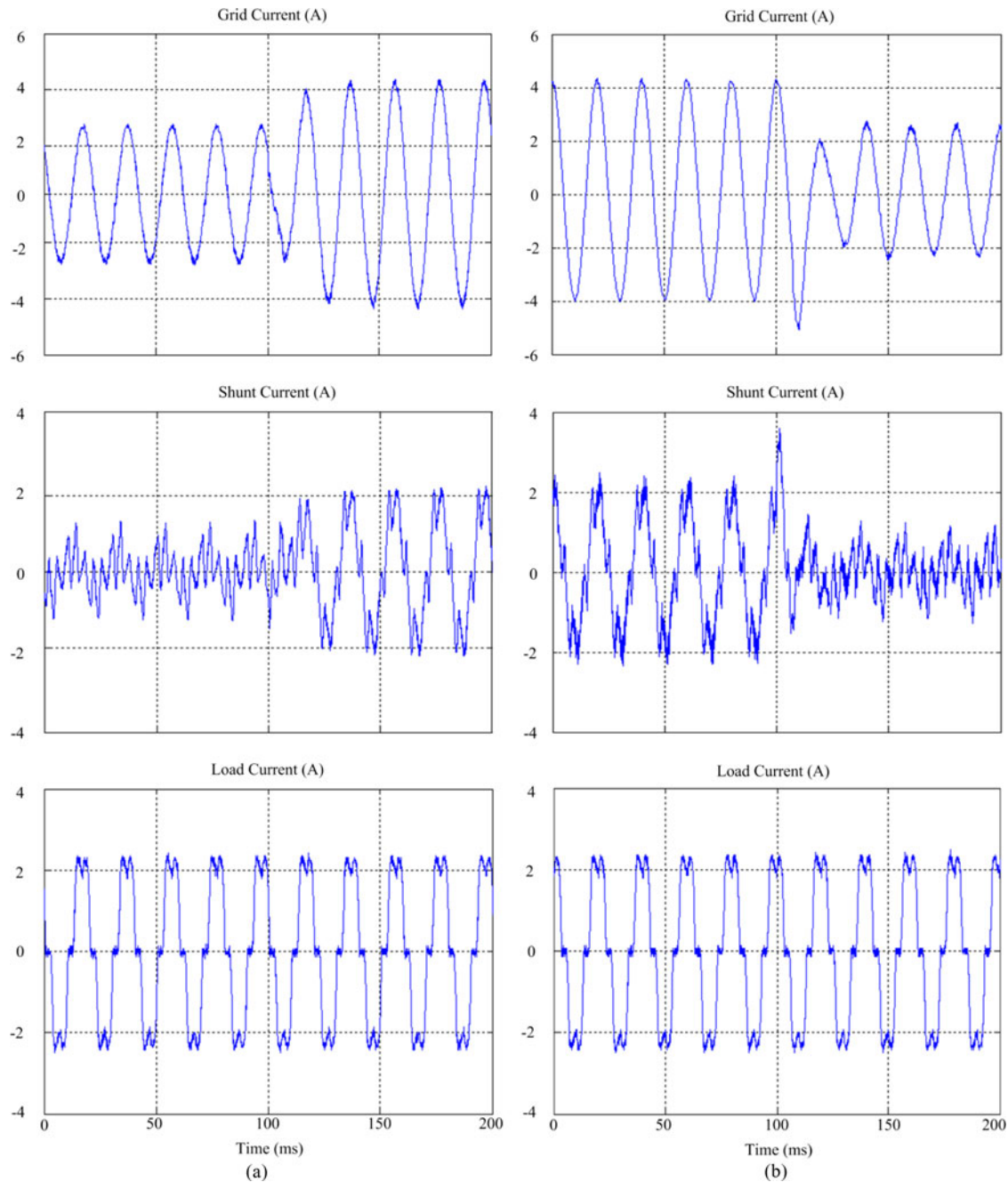
Fig. 12. Experimental grid, shunt injection, and load currents during (a) normal-to-sag and (b) sag-to-normal transitions.

throughout the whole transitional process with an increase in amplitude noted during the period of grid sag. This increase in grid current is transferred to the shunt terminal of the nine-switch power conditioner, whose absorbed (negative of injected) current now has a prominent fundamental component, as also reflected by the second row of waveforms plotted in Fig. 12. Upon processed by the nine-switch power stage, the incremental power associated with the higher shunt current is eventually forced out of the series terminal as an injected voltage, needed for keeping the load voltage and power unchanged.

Yet another feature verified through the testing is the dc-link voltage needed by the nine-switch power conditioner, whose value is always higher than that of the back-to-back conditioner, if series compensation is demanded. This increase can, however, be kept small by adopting the carrier division scheme shown in Fig. 3. To confirm that, Fig. 13 shows the conditioner dc-link voltage regulated at only 270 V throughout the whole sag and recovery process. This dc-link voltage is merely 8% higher than that of the back-to-back case, hence verifying those theoretical reasoning discussed in Sections II-C and III.
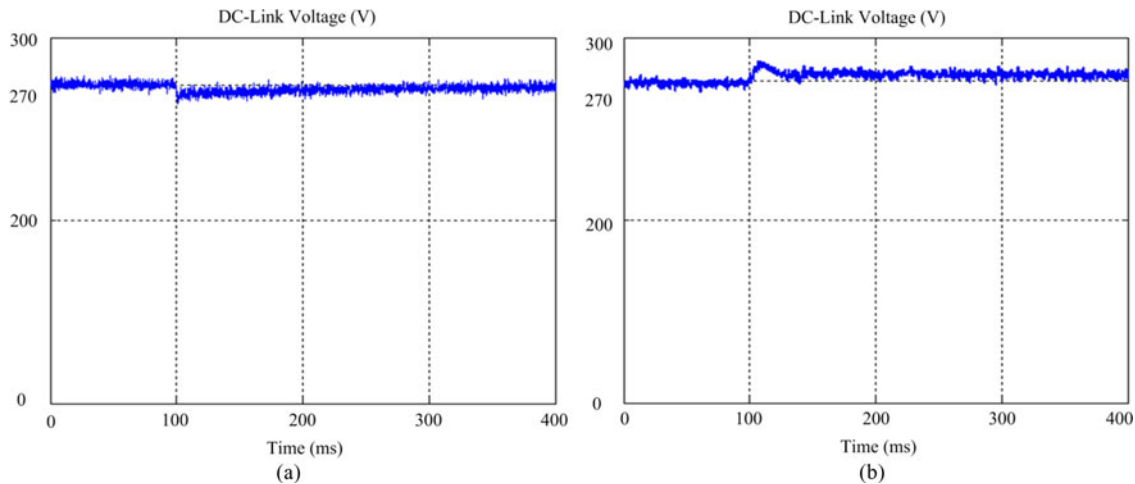
Fig. 13. Experimental dc-link voltage during (a) normal-to-sag and (b) sag-to-normal transitions.

VI. CONCLUSION

This paper evaluates shortcomings experienced by previous applications of the newly proposed nine-switch converter. With a better understanding developed, the conclusion drawn is that the nine-switch converter is not an attractive alternative for replacing back-to-back converter with two shunt bridges. Instead, the nine-switch converter is more suitable for replacing back-to-back converter in "series–shunt" systems, where one good example is the UPQC. As a further performance booster, a modified 120°-discontinuous modulation scheme is presented for reducing the overall commutation count by 33%. Followed up next with proper shunt and series control, harmonics, reactive power, and voltage sags are compensated promptly with no appreciable degradation in performance. The nine-switch conditioner is therefore proved to be effective, while yet using lesser semiconductor switches. Experimental results for confirming its anticipated smooth performance have already been obtained through intensive laboratory testing.

REFERENCES

[1] D. L. Ashcroft, "The static power converter committee—Some perspectives," *IEEE Trans. Ind. Applicat.*, vol. IA-21, no. 5, pp. 1097–1098, Sep. 1985.
[2] B. Han, B. Bae, H. Kim, and S. Baek, "Combined operation of unified power-quality conditioner with distributed generation," *IEEE Trans. Power Delivery*, vol. 21, no. 1, pp. 330–338, Jan. 2006.
[3] H. Johal and D. Divan, "Design considerations for series-connected distributed FACTS converters," *IEEE Trans. Ind. Applicat.*, vol. 43, no. 6, pp. 1609–1618, Nov./Dec. 2007.
[4] T. L. Lee, J. C. Li, and P. T. Cheng, "Discrete frequency tuning active filter for power system harmonics," *IEEE Trans. Power Electron.*, vol. 24, no. 5, pp. 1209–1217, May 2009.
[5] V. Khadkikar and A. Chandra, "A new control philosophy for a unified power quality conditioner (UPQC) to coordinate load-reactive power demand between shunt and series inverters," *IEEE Trans. Power Del.*, vol. 23, no. 4, pp. 2522–2534, Oct. 2008.
[6] Y. , W. Li, D. M. Vilathgamuwa, and P. C. Loh, "A grid-interfacing power quality compensator for three-phase three-wire microgrid applications," *IEEE Trans. Power Electron.*, vol. 21, no. 4, pp. 1021–1031, Jul. 2006.
[7] J. W. Kolar, F. Schafmeister, S. D. Round, and H. Ertl, "Novel three-phase ac–ac sparse matrix converters," *IEEE Trans. Power Electron.*, vol. 22, no. 5, pp. 1649–1661, Sep. 2007.
[8] P. C. Loh, F. Blaabjerg, F. Gao, A. Baby, and D. A. C. Tan, "Pulsewidth modulation of neutral-point-clamped indirect matrix converter," *IEEE Trans. Ind. Applicat.*, vol. 44, no. 6, pp. 1805–1814, Nov./Dec. 2008.
[9] F. Blaabjerg, S. Freysson, H. H. Hansen, and S. Hansen, "A new optimized space-vector modulation strategy for a component-minimized voltage source inverter," *IEEE Trans. Power Electron.*, vol. 12, no. 4, pp. 704–714, Jul. 1997.
[10] E. Ledezma, B. McGrath, A. Munoz, and T. A. Lipo, "Dual ac-drive system with a reduced switch count," *IEEE Trans. Ind. Applicat.*, vol. 37, no. 5, pp. 1325–1333, Sep./Oct. 2001.
[11] M. Jones, S. N. Vukosavic, D. Dujic, E. Levi, and P. Wright, "Five-leg inverter PWM technique for reduced switch count two-motor constant power applications," *IET Proc. Electric Power Applicat.*, vol. 2, no. 5, pp. 275–287, Sep. 2008.
[12] C. Liu, B. Wu, N. R. Zargari, D. Xu, and J. Wang, "A novel three-phase three-leg ac/ac converter using nine IGBTs," *IEEE Trans. Power Electron.*, vol. 24, no. 5, pp. 1151–1160, May 2009.
[13] T. Kominami and Y. Fujimoto, "A novel three-phase inverter for independent control of two three-phase loads," in *Proc. IEEE-Ind. Applicat. Soc. (IAS)s*, 2007, pp. 2346–2350.
[14] T. Kominami and Y. Fujimoto, "Inverter with reduced switching-device count for independent ac motor control," in *Proc. IEEE-IECON*, 2007, pp. 1559–1564.
[15] C. Liu, B. Wu, N. R. Zargari, and D. Xu, "A novel nine-switch PWM rectifier-inverter topology for three-phase UPS applications," in *Proc. IEEE-Everyday Practical Electron. (EPE)*, 2007, pp. 1–10.
[16] S. M. Dehghan, M. Mohamadian, and A. Yazdian, "Hybrid electric vehicle based on bidirectional Z-source nine-switch inverter," *IEEE Trans. Veh. Technol.*, vol. 59, no. 6, pp. 2641–2653, Jul. 2010.
[17] M. , J. Newman, D. G. Holmes, J. G. Nielsen, and F. Blaabjerg, "A dynamic voltage restorer (DVR) with selective harmonic compensation at medium voltage level," *IEEE Trans. Ind. Applicat.*, vol. 41, no. 6, pp. 1744–1753, Nov./Dec. 2005.
[18] M. J. Newman and D. G. Holmes, "A universal custom power conditioner (UCPC) with selective harmonic voltage compensation," in *Proc. IEEE-IECON*, 2002, pp. 1261–1266.
[19] Y. Li, D. M. Vilathgamuwa, and P. C. Loh, "Microgrid power quality enhancement using a three-phase four-wire grid-interfacing compensator," *IEEE Trans. Ind. Applicat.*, vol. 41, no. 6, pp. 1707–1719, Nov./Dec. 2005.
[20] O. Ojo, "The generalized discontinuous PWM scheme for three-phase voltage source inverters," *IEEE Trans. Ind. Electron.*, vol. 51, no. 6, pp. 1280–1289, Dec. 2004.
[21] S. M. D. Dehnavi, M. Mohamadian, A. Yazdian, and F. Ashrafzadeh, "Space vectors modulation for nine-switch converters," *IEEE Trans. Power Electron.*, vol. 25, no. 6, pp. 1488–1496, Jun. 2010.
[22] F. Gao, L. Zhang, D. Li, P. , C. Loh, Y. Tang, and H. Gao, "Optimal pulsewidth modulation of nine-switch converter," *IEEE Trans. Power Electron.*, vol. 25, no. 9, pp. 2331–2343, Sep. 2010.
[23] D. N. Zmood, D. G. Holmes, and G. H. Bode, "Frequency-domain analysis of three-phase linear current regulators," *IEEE Trans. Ind. Appl.*, vol. 37, no. 2, pp. 601–610, Mar./Apr. 2001.

[24] P. Mattavelli, "Closed-loop selective harmonic compensation for active filters," *IEEE Trans. Ind. Appl.*, vol. 37, no. 1, pp. 81–89, Jan./Feb. 2001.

[25] R. Teodorescu, F. Blaabjerg, M. Liserre, and P. C. Loh, "Proportional-resonant controllers and filters for grid-connected voltage-source converters," *IEE Proc. Electric Power Applicat.*, vol. 153, no. 5, pp. 750–762, Sep. 2006.

[26] D. N. Zmood and D. G. Holmes, "Stationary frame current regulation of PWM inverters with zero steady-state error," *IEEE Trans. Power Electron.*, vol. 18, no. 3, pp. 814–822, May 2003.

Feng Gao (S'07–M'09) received the B.Eng. and M.Eng. degrees in electrical engineering from Shandong University, Jinan, China, in 2002 and 2005, respectively, and the Ph.D. degree from the School of Electrical and Electronic Engineering, Nanyang Technological University, Singapore, in 2009.

From 2008 to 2009, he was a Research Fellow in Nanyang Technological University. Since 2010, he joined the School of Electrical Engineering, Shandong University, where he is currently a Professor. From September 2006 to February 2007, he was a Visiting Scholar at the Institute of Energy Technology, Aalborg University, Aalborg, Denmark.

Dr. Gao was the recipient of the IEEE Industry Applications Society Industrial Power Converter Committee Prize for a paper published in 2006.

Lei Zhang received the Bachelor's degree in electrical engineering in 2007 from Wuhan University, Wuhan, China. From 2007 to 2008, he studied in Power Engineering in Chalmers University of Technology, Gothenburg, Sweden. Currently, he is working toward the Ph.D. degree from the School of Electrical and Electronic Engineering, Nanyang Technological University, Singapore.

From July to October in 2009, he was a Visiting Scholar in the Institute of Energy Technology, Aalborg University, Denmark, where he worked on the HVdc system in RTDS simulator. His research field includes distributed control of multiple converters, renewable technology, and converter design.
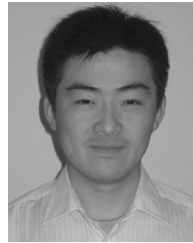
Poh Chiang Loh (S'01–M'04) received the B.Eng. (Hons.) and M.Eng. degrees from the National University of Singapore in 1998 and 2000, respectively, and the Ph.D. degree from Monash University, Australia, in 2002, all in electrical engineering.

During the summer of 2001, he was a Visiting Scholar with the Wisconsin Electric Machine and Power Electronics Consortium, University of Wisconsin-Madison, Madison, where he worked on the synchronized implementation of cascaded multilevel inverters, and reduced common mode carrier-based and hysteresis control strategies for multilevel inverters. From 2002 to 2003, he was a Project Engineer with the Defence Science and Technology Agency, Singapore, managing major defence infrastructure projects and exploring new technology for defence applications. From 2003 to 2009, he was an Assistant Professor with the Nanyang Technological University, Singapore, and since 2009, he has been an Associate Professor at the same university. In 2005, he has been a Visiting Staff first at the University of Hong Kong, and then at Aalborg University, Denmark. In 2007 and 2009, he again returned to Aalborg University first as a Visiting Staff working on matrix converters and the control of grid-interfaced inverters, and then as a Guest Member of the Vestas Power Program.

Dr. Loh has received two-third paper prizes from the IEEE-IAS IPCC committee in 2003 and 2006, and he is now serving as an Associate Editor of the IEEE TRANSACTIONS ON POWER ELECTRONICS.